Noise-induced mixed-mode oscillations in a relaxation oscillator near the onset of a limit cycle

Cyrill B. Muratov
Department of Mathematical Sciences, New Jersey Institute of Technology, Newark, New Jersey 07102, USA

Eric Vanden-Eijnden
Courant Institute of Mathematical Sciences, New York University, New York, New York 10012, USA

(Received 21 February 2007; accepted 15 June 2007; published online 27 March 2008)

A detailed asymptotic study of the effect of small Gaussian white noise on a relaxation oscillator undergoing a supercritical Hopf bifurcation is presented. The analysis reveals an intricate stochastic bifurcation leading to several kinds of noise-driven mixed-mode oscillations at different levels of amplitude of the noise. In the limit of strong time-scale separation, five different scaling regimes for the noise amplitude are identified. As the noise amplitude is decreased, the dynamics of the system goes from the limit cycle due to self-induced stochastic resonance to the coherence resonance limit cycle, then to bursting relaxation oscillations, followed by rare clusters of several relaxation cycles (spikes), and finally to small-amplitude oscillations (or stable fixed point) with sporadic single spikes. These scenarios are corroborated by numerical simulations. © *2008 American Institute of Physics*. [DOI: 10.1063/1.2779852]

This paper investigates the effect of small random perturbations of dynamical systems near the onset of relaxation limit cycle oscillations. Such problems often arise in a wide range of applications in physics, chemistry, and, especially, biology, where the emergence of a limit cycle marks the transition from excitable to oscillatory behavior. An important feature of the systems under consideration is the presence of a strong time-scale separation between the dynamics of their components. This multiscale nature makes the dynamics particularly insensitive to noise, offering a generic and robust way of generating rhythmic activities. Yet it was recently found that noise can lead to surprising new effects in systems whose deterministic dynamics are characterized by the existence of fast and slow motions. Remarkably, in these systems noise can result in new dynamics that are highly coherent, yet distinct from the dynamics observed in the absence of the noise. Such phenomena require the "right" amount of noise: if the noise amplitude is too large, the noise will wipe out any coherent dynamics; if, on the other hand, the amplitude of the noise is too small, then it will have a negligible effect. Here we study the role of the noise amplitude in a system near the threshold to relaxation limit cycle oscillations. We find that noise has an intricate interplay with the deterministic dynamics in the vicinity of the fixed point, which is about to lose its stability. Different amounts of noise lead to qualitatively distinct behaviors, making the transition from excitability to relaxation oscillations highly nontrivial. We argue that the predicted phenomena must be inevitable in real excitable systems as noise is always present in noticeable amounts in such systems.

I. INTRODUCTION

Limit cycle oscillations are universally encountered in a variety of nonlinear dynamical systems modeling an enormous range of applications in the natural sciences and engineering (see, e.g., Refs. 1–5). They come in all kinds of "shapes and sizes," yet one mechanism is particularly important for the robust generation of limit cycle oscillations. This mechanism relies on a strong separation of time scales between different dynamical components of the system and gives rise to an important special class of nonlinear dynamical systems, namely relaxation oscillators.[6–8] In the first approximation, a relaxation oscillator can be thought of as a hybrid dynamical system in which the slow dynamics are governed by the motions restricted to the slow manifold. These slow motions must be supplemented by the rules governing fast (instantaneous on the slow time scale) jumps between certain portions on the slow manifold.[6,9] This geometric picture is typically adequate for the description of the system's dynamics away from bifurcation points.

Relaxation oscillations are a remarkably robust phenomenon, due to the geometric nature of their underlying mechanism, and as such should be expected to be particularly insensitive to noise. This is probably why relaxation oscillators are encountered so often in biological systems where noise is often present in noticeable amounts.[5,10–12] Yet recent studies have found quite surprising and unexpected behaviors of relaxation oscillators in the presence of even relatively small amounts of noise.[12–19] Importantly, noise has been shown to alter the dynamics of the system while actually producing very little randomness. In other words, noise was demonstrated to be able to play a *constructive* role in the dynamics of nonlinear systems with multiple time scales.

One mechanism, referred to as coherence resonance (CR), has been shown to result in the onset of a large-amplitude relaxation limit cycle in systems that are about to undergo a Hopf bifurcation[11,14] (for an extensive review, see Ref. 20). In such systems, the noise plays the role to uncover the precursor to the large-amplitude limit cycle about to be created past the bifurcation threshold.[21] Perhaps even more surprisingly, under certain conditions small noise has been demonstrated to lead to the onset of an entirely new oscillatory behavior as a result of the mechanism referred to as self-induced stochastic resonance (SISR).[17,18,21–25] Remarkably, the degree of coherence of the dynamics is under control within SISR, i.e., it can be made arbitrarily high by a suitable choice of the parameters without affecting the limiting deterministic dynamics. Moreover, this choice of the parameters does not require fine-tuning, making the mechanism robust and generic.

SISR persists near a Hopf bifurcation, with smaller amounts of noise necessary to produce the effect similar to CR.[21] As the bifurcation is approached, the interplay between the deterministic dynamics and the noise can become quite intricate, due to a singular character of the Hopf bifurcation in systems with strong time-scale separation.[26–29] In this paper, we investigate the detailed structure of the Hopf bifurcation in a relaxation oscillator perturbed by noises of different amplitudes in relationship to the time-scale separation ratio. To be specific, we focus on the classical FitzHugh-Nagumo system perturbed by additive Gaussian white noise. We verified that the main scenarios described in this paper are not system-specific and can be observed, e.g., in the noise-driven Morris-Lecar model of a type-II neuron (for a recent study of this model, see Ref. 30). We develop an asymptotic theory of noise-driven relaxation oscillators and verify the obtained picture through numerical simulations. Due to the universal character of the Hopf bifurcation in relaxation oscillators,[29] our results are expected to be applicable to a general class of nonlinear dynamical systems with fast and slow subsystems in the presence of noise.

The model under study is the following systems of stochastic differential equations (SDEs):

$$\varepsilon\dot{x} = x - \tfrac{1}{3}x^3 - y + \sqrt{\varepsilon}\delta_1\dot{W}_1, \tag{1a}$$

$$\dot{y} = x + a + \delta_2\dot{W}_2. \tag{1b}$$

Here, x and y are the dynamical variables, ε, δ_1, δ_2, and a are positive parameters, and W_1 and W_2 are independent Wiener processes. We assume throughout the paper that $\varepsilon \ll 1$, implying that x is fast and y is slow. We are also interested in the situation in which the noise amplitude is small. More precisely, we define the parameter

$$\delta = \sqrt{\delta_1^2 + \delta_2^2} \ll 1, \tag{2}$$

which characterizes the strength of the stochastic perturbation. Indeed, the value of δ controls the noise strength in both equations in Eqs. (1a) and (1b) on their corresponding time scales, which are $O(\varepsilon)$ and $O(1)$, respectively. In the following, we will investigate different scaling regimes as $\varepsilon \to 0$ with $\delta \to 0$ jointly on appropriate sequences. Depending on the choice of the sequence, a rich variety of qualitatively different behaviors will be demonstrated.

This paper is organized as follows. In Sec. II, we review the analysis of the solutions of Eqs. (1a) and (1b) in an $O(\varepsilon)$ neighborhood of the Hopf bifurcation (in terms of the parameter a) in the absence of noise. Then, in Sec. III, we derive a reduced one-dimensional SDE describing the behavior of the solution near the fixed point in the presence of sufficiently small noise. In Sec. IV, we interpret the solutions of the reduced problem from the preceding section in various scaling limits. In Sec. V, we corroborate the conclusions of the asymptotic analysis via numerical simulations of Eqs. (1a) and (1b). Finally, in Sec. VI, we summarize the results of our analysis and discuss its possible implications to applications.

II. SINGULAR HOPF BIFURCATION

Let us first discuss the onset of the limit cycle oscillations in the deterministic version of Eqs. (1a) and (1b), i.e., when $\delta \equiv 0$. The analysis of the deterministic version of system (1a) and (1b) shows that it has a unique fixed point,

$$x_0 = -a, \quad y_0 = -a + \tfrac{1}{3}a^3, \tag{3}$$

which is stable for $|a| > 1$, while at $|a| = 1$ the system undergoes a Hopf bifurcation. In both cases, the bifurcation is supercritical, with the frequency of the quasiharmonic oscillations at the onset being $\omega_0 = \varepsilon^{-1/2}$. Note that because of the symmetry $x \to -x$, $y \to -y$, and $a \to -a$, it is sufficient to study the behavior of the system only near one bifurcation point, say $a = 1$.

For $\varepsilon \ll 1$, the Hopf bifurcation acquires a singular character, and so the normal form expansion near the point $a = 1$ remains valid only in a very narrow range of a. Nevertheless, the dynamics near this singular Hopf bifurcation can be completely characterized asymptotically and does not depend on the detailed features of the nonlinearities. A general asymptotic analysis of the onset of the limit cycle in the vicinity of a Hopf bifurcation in two-variable dynamical systems in the limit $\varepsilon \to 0$ was performed by Baer and Erneux.[26,27] They identified a range of the bifurcation parameter $1 - a = O(\varepsilon)$ in which the limit cycle emerging past the bifurcation threshold changes from small-amplitude oscillations, whose amplitudes in x and y are $O(\varepsilon^{1/2})$ and $O(\varepsilon)$, respectively, to a relaxation limit cycle whose amplitude is $O(1)$ in both x and y. The transition to the $O(1)$ limit cycle occurs via the "canard explosion" in an exponentially narrow range of the parameter a within an ε-neighborhood of the bifurcation threshold.[6,31,32] A computation shows that in the particular system considered here, the transition to relaxation oscillations occurs asymptotically at $1 - a = \frac{1}{8}\varepsilon$ (see below).[26]

Past this transition region, the limit cycle is essentially that shown in Fig. 1.[1,6,9] It consists of the slow motions down and up the left and the right branches of the slow manifold $S = S_L \cup S_R$, where

$$S_L = \left\{(x,y): x \in (-\infty, -1), y = x - \tfrac{1}{3}x^3\right\}, \tag{4}$$

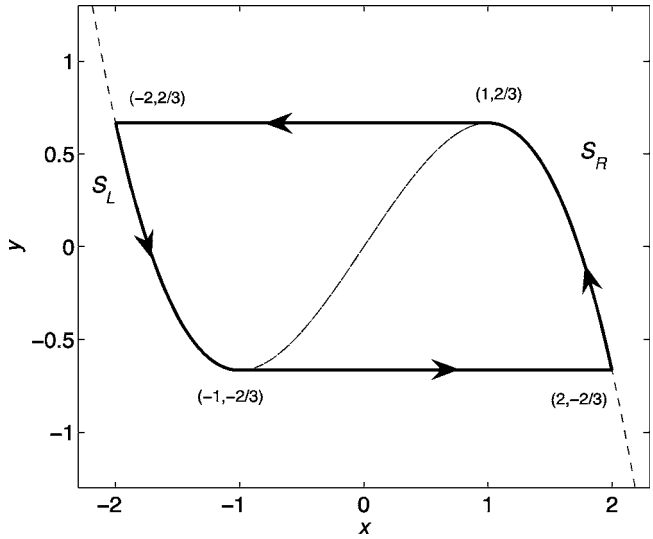

FIG. 1. The relaxation limit cycle. The dashed line is the curve $y=x-\frac{1}{3}x^3$.

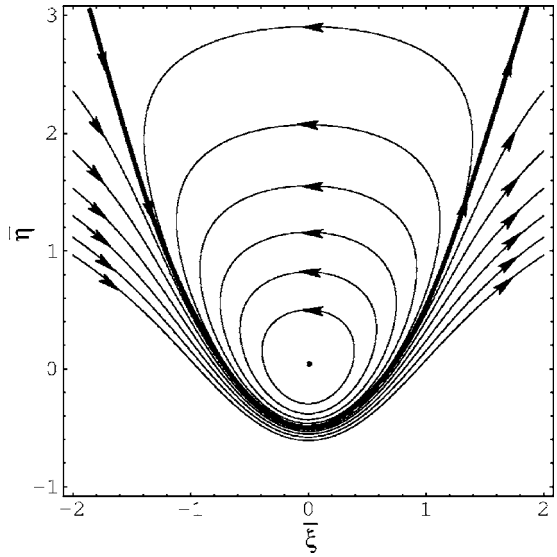

FIG. 2. The phase portrait of the reduced system. The thick solid line is the separatrix.

$$S_R=\left\{(x,y):x\in(+1,+\infty),y=x-\tfrac{1}{3}x^3\right\}, \tag{5}$$

connected by fast transitions from S_R to S_L or vice versa. The transition from S_R to S_L occurs when the trajectory reaches the right knee at $(x,y)=\left(1,\frac{2}{3}\right)$; during the transition, the value of y remains asymptotically constant. Similarly, the transition from S_L to S_R occurs when the trajectory reaches the left knee on the slow manifold at $(x,y)=\left(-1,-\frac{2}{3}\right)$. This limit cycle persists when $\varepsilon\to 0$ first and then $a\to 1^-$ afterwards. In this case, the time to reach the left knee on S_L remains finite despite the fact that in the limit the fixed point (x_0,y_0) is located right at the knee. The period of the limit cycle (LC) in this limit can be calculated asymptotically: $T_{\mathrm{LC}}\simeq 3$, see Ref. 21. Let us emphasize that in the absence of noise, the system possesses a unique global attractor (either the fixed point for $|a|\geq 1$ or the limit cycle for $|a|<1$). Hence, for all values of the parameters there is no bistability in the considered problem with $\delta=0$, and so at vanishingly small noise amplitudes the trajectories of the system go to the attractor with probability 1.[33]

III. STOCHASTIC EXTENSION

We are interested in how the noise added to the right-hand side of Eqs. (1a) and (1b), i.e., the case of $\delta>0$ changes the zero-noise picture. In what follows, we will use the ideas of Baer and Erneux applied to the system of *stochastic* differential equations near the onset of a singular Hopf bifurcation and develop an asymptotic theory of the noise-driven singular Hopf bifurcation.

A. Dynamics in the vicinity of the fixed point

Following the ideas of Baer and Erneux,[26,27] we introduce the rescaled variables, together with new time and the control parameter,

$$\xi=\varepsilon^{-1/2}(x-x_0),\quad \eta=\varepsilon^{-1}(y-y_0), \tag{6}$$

$$\tau=\varepsilon^{-1/2}t,\quad \mu=\varepsilon^{-1}(1-a). \tag{7}$$

In terms of these variables, Eqs. (1a) and (1b) can be rewritten as the following systems of SDEs:

$$d\xi=\left\{\xi^2-\eta+\varepsilon^{1/2}\left(2\mu\xi-\tfrac{1}{3}\xi^3\right)\right\}d\tau+\delta_1\varepsilon^{-3/4}dW_1(\tau)+\cdots, \tag{8a}$$

$$d\eta=\xi d\tau+\delta_2\varepsilon^{-3/4}dW_2(\tau), \tag{8b}$$

where "$\cdots$" denotes higher-order terms in ε.

Observe that in the limit $\varepsilon\to 0$, $\varepsilon^{-3/4}\delta\to 0$, the system (8a) and (8b) reduces to a pair of ordinary differential equations. Denoting by $\bar{\xi}$ and $\bar{\eta}$ the solution of Eqs. (8a) (8b) in this limit, we have

$$\frac{d\bar{\xi}}{d\tau}=\bar{\xi}^2-\bar{\eta}, \tag{9a}$$

$$\frac{d\bar{\eta}}{d\tau}=\bar{\xi}. \tag{9b}$$

By inspection, one sees that this system admits a first integral,

$$G=e^{-2\eta}(1+2\eta-2\xi^2), \tag{10}$$

i.e., we have $(d/d\tau)G(\bar{\xi},\bar{\eta})\equiv 0$. For $0<G<1$, all trajectories of Eqs. (9a) and (9b) are closed curves corresponding to cycles, whereas for $G<0$ all trajectories are unbounded, going from $\xi=-\infty$ to $\xi=+\infty$ (see Fig. 2). The trajectory corresponding to $G=0$,

$$\bar{\eta}=\bar{\xi}^2-\tfrac{1}{2}, \tag{11}$$

is the separatrix between these two classes of solutions. Finally, the solution corresponding to $G=1$ is the fixed point, $\bar{\xi}=0$, $\bar{\eta}=0$.

Going back to the original system of SDEs in Eqs. (8a) and (8b), one can see that G will be a slowly varying quan-

tity for $\varepsilon \ll 1$ and $\varepsilon^{-3/4}\delta \ll 1$. Applying the Itô formula[34] to G with ξ and η from Eqs. (8a) and (8b), we obtain

$$dG = -2\varepsilon^{1/2}e^{-2\eta}\Big\{\xi^2\Big(4\mu - \tfrac{2}{3}\xi^2\Big) + \varepsilon^{-2}[\delta_1^2 + \delta_2^2(2\xi^2 - 2\eta + 1)]\Big\}d\tau + 4\varepsilon^{-3/4}e^{-2\eta}\sqrt{\delta_1^2\xi^2 + \delta_2^2(\xi^2-\eta)^2}\,dW(\tau) + \cdots, \quad (12)$$

where, again, "$\cdots$" denote higher-order terms. Now, to obtain a closed equation for the leading-order approximation to G, denoted by $\bar{G}$, for $0<G<1$, we average Eq. (12) with $\xi=\bar{\xi}$ and $\eta=\bar{\eta}$ over a period of the cycle.[33] This leads to the following asymptotic SDE for $\bar{G}$:

$$d\bar{G} = b(\bar{G})d\tau + \sigma(\bar{G})dW(\tau), \quad (13)$$

with a natural boundary condition at $\bar{G}=1$ and an absorbing (since for $G<0$ the solutions run off to infinity) boundary condition at $\bar{G}=0$. The effective drift and dispersion terms in Eq. (13) are given explicitly by

$$b = -\frac{2\varepsilon^{1/2}}{T}\int_0^T e^{-2\bar{\eta}}\Big\{\bar{\xi}^2\Big(4\mu - \tfrac{2}{3}\bar{\xi}^2\Big) + \varepsilon^{-2}[\delta_1^2 + \delta_2^2(2\bar{\xi}^2 - 2\bar{\eta} + 1)]\Big\}d\tau, \quad (14)$$

$$\sigma^2 = \frac{16\varepsilon^{-3/2}}{T}\int_0^T e^{-4\bar{\eta}}\{\delta_1^2\bar{\xi}^2 + \delta_2^2(\bar{\xi}^2 - \bar{\eta})^2\}d\tau, \quad (15)$$

where $T=T(\bar{G})$ is the period of the cycle with $G=\bar{G}$. Using Eqs. (9a) and (9b), one easily finds

$$T = 2\int_{\eta_{\min}(\bar{G})}^{\eta_{\max}(\bar{G})}\frac{d\bar{\eta}}{|\bar{\xi}|}, \quad \bar{\xi} = \pm\sqrt{\frac{1+2\bar{\eta}-\bar{G}e^{2\eta}}{2}}. \quad (16)$$

Let us now analyze Eq. (13) in more detail. First of all, observe that by assumption $\bar{G}\in(0,1)$. According to Eqs. (14) and (15), in the vicinity of $\bar{G}=1$ we have

$$T \simeq 2\pi, \quad (17)$$

$$b \simeq -2\varepsilon^{1/2}\{\mu(1-\bar{G}) + \varepsilon^{-2}(\delta_1^2+\delta_2^2)\}, \quad (18)$$

$$\sigma^2 \simeq 4\varepsilon^{-3/2}(\delta_1^2+\delta_2^2)(1-\bar{G}), \quad (19)$$

where we have expanded $\bar{\xi}$ and $\bar{\eta}$ around $(\bar{\xi},\bar{\eta})=(0,0)$. Similarly, in the vicinity of $\bar{G}=0$ we have

$$T \simeq 4\ln^{1/2}\bar{G}^{-1/2}, \quad (20)$$

$$b \simeq \sqrt{\frac{\pi e^2}{2\varepsilon^3\ln\bar{G}^{-1/2}}}[\varepsilon^2(\mu^*-\mu) - \delta_1^2 - 2\delta_2^2], \quad (21)$$

$$\sigma^2 \simeq \sqrt{\frac{\pi e^4}{4\varepsilon^3\ln\bar{G}^{-1/2}}}(\delta_1^2 + 2\delta_2^2), \quad (22)$$

where now we took into account that for $\bar{G}\ll 1$ the trajectory $(\bar{\xi}(\tau),\bar{\eta}(\tau))$ spends most of its time in the neighborhood of the separatrix in Eq. (11), and that $T\gg 1$. In Eq. (21),

$$\mu^* = \tfrac{1}{8}, \quad (23)$$

which is the critical value of μ at which the small-amplitude limit cycle disappears via the "canard explosion" phenomenon for $\delta=0$ in the limit $\varepsilon\to 0$; see Refs. 6, 26, 27, 31, and 32.

In general, the functions $b(\bar{G})$ and $\sigma(\bar{G})$ can be represented as

$$b(\bar{G}) = \varepsilon^{-3/2}\{b_1(\bar{G})\delta_1^2 + b_2(\bar{G})\delta_2^2\} + \varepsilon^{1/2}\{b_3(\bar{G})\mu + b_4(\bar{G})\}, \quad (24)$$

$$\sigma^2(\bar{G}) = \varepsilon^{-3/2}\{\sigma_1^2(\bar{G})\delta_1^2 + \sigma_2^2(\bar{G})\delta_2^2\}, \quad (25)$$

where the dependence of b_i's and σ_i's on $\bar{G}$ can be found numerically by evaluating the corresponding integrals in Eqs. (14) and (15), making use of Eq. (16). These dependences are plotted in Fig. 3. Let us note that outside of the immediate vicinity of $\bar{G}=0$ these quantities can be very well approximated by the following expressions: $b_1\approx -2+\frac{1}{10}(1-\bar{G})^2$, $b_2\approx -4+2\bar{G}$, $b_3\approx 2(\bar{G}-1)$, $b_4\approx\frac{1}{7}(1-\bar{G})^2$, $\sigma_1^2\approx 4(1-\bar{G})$, and $\sigma_2^2\approx 6(1-\bar{G})$.

The representation in Eqs. (24) and (25) also allows one to construct the potential

$$V(\bar{G}) = -\frac{2\delta^2}{\varepsilon^2}\int\frac{b(\bar{G})}{\sigma^2(\bar{G})}d\bar{G}. \quad (26)$$

At small effective noise amplitudes, $\delta/\varepsilon\ll 1$, this potential becomes independent of δ and ε and determines the behavior of metastable equilibria governed by Eq. (13). In particular, the metastable probability density for $\bar{G}$ is given by

$$\bar{p}(\bar{G}) \propto \exp[-\varepsilon^2 V(\bar{G})/\delta^2]. \quad (27)$$

Also, the lifetime of the metastable state $\bar{G}^*$ corresponding to the minimum of V is, to the leading order, determined by the barrier $\Delta V = V(0) - V(\bar{G}^*)$, and is $O[\exp(\varepsilon^2\Delta V/\delta^2)]$ for $\Delta V>0$, see Ref. 33.

An example of the form of V for one choice of the parameters is shown in Fig. 4. Here the potential V has a global minimum at $\bar{G}^*\approx 0.8$, corresponding to the stable fixed point, and $\bar{p}(\bar{G})$ is concentrated in the vicinity of the fixed point. Also note that $dV/d\bar{G}<0$ strictly at $\bar{G}=0$. The latter is, in fact, true for all $\mu<\mu^*-\varepsilon^{-2}(\delta_1^2+2\delta_2^2)$.

B. Matching conditions

We now discuss how the dynamics in the vicinity of the fixed point (x_0,y_0) is connected with the global dynamics in the presence of large excursions away from the fixed point. Suppose that we are given an initial condition that is $O(1)$ away from the fixed point (here we use the original, unscaled, variables and time). Then the initial stage of the dynamics will be governed by the fast motions in which the value of y is frozen. The noise will have a small effect on this dynamics for $\delta\ll 1$. As a result, on the $O(\varepsilon)$ time scale, the trajectory of the system is initially attracted to the stable manifold S consisting of the left and the right branch, S_L and

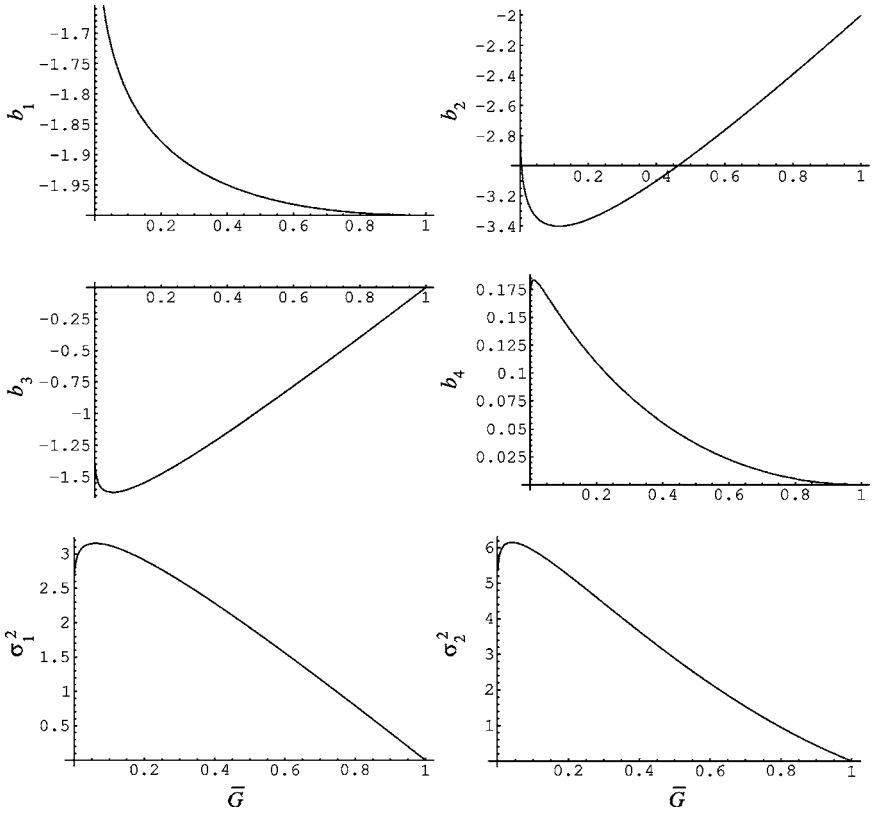

FIG. 3. The dependences of the functions b_i's and σ_i's on $\bar{G}$.

S_R, respectively [see Eqs. (4) and (5), and Fig. 1], depending on the initial value of x. After that, the trajectory will follow the slow manifold on the $O(1)$ time scale of the slow motions. For $\mu=O(1)$, we may set $a=1$ to the leading order in ε in order to describe the slow motions away from the immediate vicinity of the fixed point.

Assuming that $\delta_1^2 \ln \varepsilon^{-1} \ll 1$, i.e., that we are not dealing with SISR,[21] the slow dynamics can proceed according to two scenarios. If the trajectory initially falls on S_R, it first moves up S_R to reach the right knee at $(x,y)=(1,\frac{2}{3})$, then jumps to S_L, and then proceeds down S_L toward the left knee at $(x,y)=(-1,-\frac{2}{3})$. Or, the trajectory will immediately proceed down S_L toward the left knee, if it started on S_L at the beginning. In both cases, the trajectory eventually makes it into the vicinity of the fixed point. Importantly, it approaches the fixed point along S_L, which in this region can be approximated as $y \simeq -\frac{2}{3}+(x+1)^2$. Therefore, in terms of the scaled variables (ξ,η), the trajectory approaches the fixed point essentially along the separatrix in Eq. (11) down from $(\xi,\eta)=(-\infty,+\infty)$. In other words, when studying the dynamics of $\bar{G}$, one needs to assume that initially $\bar{G} \simeq 0$ in order to match the motions described by Eq. (13) to the large-amplitude slow motions. In terms of probability, one needs to assume that the initial probability density $p_0(\bar{G})$ upon entering the vicinity of the fixed point is given by

$$p_0(\bar{G}) = \delta(\bar{G}-0^+). \tag{28}$$

A trajectory that enters along the separatrix may leave the neighborhood of the fixed point in $O(\varepsilon^{1/2})$ time (in the original units) by escaping toward $(\xi,\eta)=(+\infty,+\infty)$, or it can get trapped in the vicinity of the fixed point. Note, however, that we cannot use Eq. (13) directly to analyze the escape statistics, since the trajectory starts initially in the immediate vicinity of the absorbing boundary. Instead, we need to look at the discrete version of Eq. (12) describing the dynamics of G on the sequence of times $\tau_n=nT$, where the period of the cycle T can be treated asymptotically as constant because of only slow logarithmic dependence on G [see Eq. (20)].

To calculate the probability density $p_n(\bar{G})$ that the trajectory remains in the vicinity of the fixed point with the value of $G(\tau_n)=\bar{G}>0$ after n revolutions around the fixed point, we look at the small change of G for $0<G\ll 1$ during each cycle. According to Eq. (12) averaged over a period, the increment of G during one cycle is asymptotically a Gaussian random variable with mean bT and dispersion $\sigma^2 T$, where b and σ^2 are given by Eqs. (21) and (22). Under these

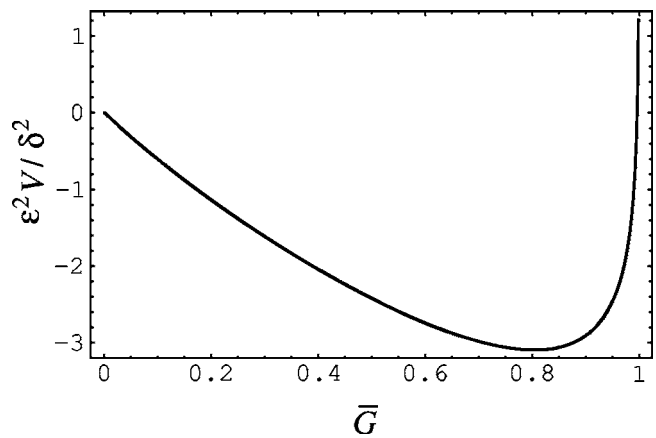

FIG. 4. The potential V computed for $\delta_1=0.1\varepsilon$, $\delta_2=0.1\varepsilon$, and $\mu=-0.1$.

assumptions, the probability density p_n is asymptotically given by

$$p_n(\bar{G}) \simeq \frac{\varepsilon^{3/4}}{2e\pi^{3/4}\sqrt{\delta_1^2+2\delta_2^2}}\int_0^\infty e^{-\{G-G'-2e\sqrt{2\pi}[\varepsilon^{1/2}(\mu^*-\mu)-\varepsilon^{-3/2}(\delta_1^2+2\delta_2^2)]\}^2/4e^2\sqrt{\pi}\varepsilon^{-3/2}(\delta_1^2+2\delta_2^2)}p_{n-1}(\bar{G}')d\bar{G}'. \tag{29}$$

Here we also assumed that the integral is dominated by a small neighborhood of $\bar{G}=0$ and extended the upper limit of integration to infinity. Note that for this to be true we must have $\delta \ll \varepsilon^{3/4}$, which is, of course, also the underlying assumption of the averaging approach of Sec. III A.

It may happen in a particular realization of the trajectory that G becomes negative for ξ large positive; such a trajectory will then run off to infinity to produce a large excursion. Therefore, the part of p_n with $\bar{G}<0$ in Eq. (29) is responsible for this phenomenon, and so the probability r_n that the trajectory escapes during the nth cycle and the total probability r of escape after any number of cycles are

$$r_n \simeq \int_{-\infty}^0 p_n(\bar{G})d\bar{G}, \quad r=\sum_{n=1}^\infty r_n, \tag{30}$$

respectively. Correspondingly, the probability that the trajectory will spend a significant amount of time in the vicinity of the fixed point is equal to $1-r$. Note that from Eq. (28) we explicitly have

$$r_1 \simeq \frac{1}{2}\left\{\mathrm{erf}\left(\frac{2^{1/2}\pi^{1/4}[\delta_1^2+2\delta_2^2+\varepsilon^2(\mu-\mu^*)]}{\varepsilon^{3/4}\sqrt{\delta_1^2+2\delta_2^2}}\right)+1\right\}, \tag{31}$$

which also gives a lower bound for r. In general, however, it is not possible to express r_n for $n>1$ in closed form. Nevertheless, it is not difficult to see that when $-\mu \gtrsim \varepsilon^{-5/4}\delta$, the series in Eq. (30) rapidly converges, and so the value of r can be significantly different from unity. It is also possible to estimate r as it approaches unity by replacing the discrete time random walk for G after a few steps by a continuous one with an absorbing boundary condition at $G=0$; the result is $1-r \sim \varepsilon^{5/4}|\mu|/\delta \ll 1$ for $-\mu \gtrsim 1$ and sufficiently large δ.

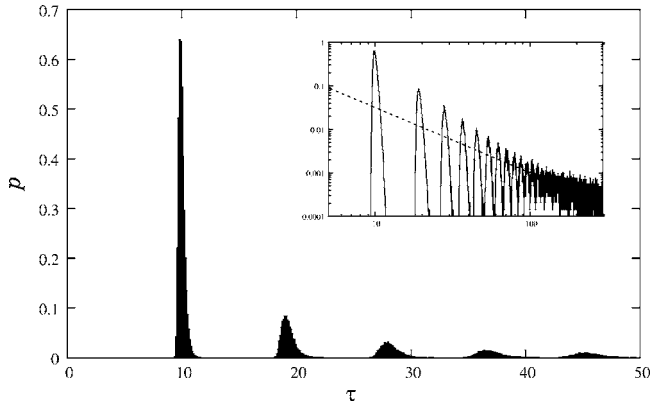

FIG. 5. The probability distribution of exit times for a trajectory satisfying Eqs. (8a) and (8b), which starts at $\xi=\xi_0$ on the separatrix and stops upon reaching $\xi=-\xi_0 \gg 1$. The inset shows the same data plotted on the log-log scale; dashed line shows the $\tau^{-3/2}$ dependence. The parameters are $\varepsilon=10^{-4}$, $\delta_1=2\times10^{-6}$, $\delta_2=0$, $\mu=0.1$, and $\xi_0=-3$. The time step of the simulation was chosen to be $\Delta\tau=10^{-4}$. The distribution is obtained from 10^5 independent runs, with each run terminated at $\tau=300$ if the trajectory failed to exit. For details of the numerical method, see Sec. V.

We verified the above picture numerically by solving Eqs. (8a) and (8b) (with higher-order terms dropped) with the initial condition (ξ_0, η_0) lying on the separatrix, with ξ_0 sufficiently large negative, and observing the trajectory until it reaches a sufficiently large positive value of ξ at which the probability of the trajectory returning to the vicinity of the origin is negligible. The probability distribution of exit times computed for a particular set of parameters chosen so that $\delta=O(\varepsilon^{5/4})$ and $\mu=O(1)$ is presented in Fig. 5. One can see that this distribution has the form of a sequence of sharp narrow peaks corresponding to exits after an integer number of revolutions in the phase plane (cf. Ref. 35). Also observe that the exit probability for a given number of revolutions initially decays algebraically (see the inset), signifying a diffusion-dominated regime. This should be followed by an exponential cutoff at $\tau \gtrsim \sigma^2 T/b^2$. Furthermore, we found that in the simulations of Fig. 5 we have $r \simeq 0.75$, which is significantly different from unity, in agreement with the theoretical arguments presented earlier. We also found $r_1 \simeq 0.383$ in the numerics, which agrees very well with the value of $r_1 \simeq 0.3716$ obtained from Eq. (31).

IV. SCALINGS

Now we are going to consider different dynamical regimes arising for different scaling relationships between δ and ε as both tend jointly to zero. Let us point out that our analysis goes beyond a direct application of the Wentzell-Freidlin large deviation theory for dynamical systems weakly perturbed by noise, since this theory is asymptotic for $\delta \to 0$ with ε fixed.[33] In all cases below, we assume that $\varepsilon \to 0$, making the standard Wentzell-Freidlin theory inapplicable.

It turns out to be convenient to consider the different scalings of δ with ε in *decreasing* order. This is because at sufficiently high noise amplitudes (for precise scalings, see below) the presence of the Hopf bifurcation becomes irrelevant as a consequence of either the SISR or the CR mechanism. As the value of δ is lowered, however, these two mechanisms are no longer realized, and the effect of the noise becomes rather intricately intertwined with the deterministic Hopf bifurcation. We investigate this interplay in detail below.

A. Self-induced stochastic resonance: $\delta_1 \lesssim \ln^{-1/2}\varepsilon^{-1}$, $\delta_2 \ll 1$

This regime was studied by us previously in Ref. 21. Here we briefly recall our main observations. When δ_2 is

sufficiently small and $\beta=\delta_1^2 \ln \varepsilon^{-1} \in (\beta_{c1}(a), \frac{3}{4})$, where $\beta_{c1}=O[(a-1)^3]$ for $1<a<\sqrt{3}$ and $\beta_{c1}=0$ for $0<a\leq 1$, a deterministic limit cycle with period $T_{\mathrm{LC}}=T_{\mathrm{SISR}}(a,\beta)$ due to SISR is created in the limit $\delta, \varepsilon \to 0$ with $\beta=O(1)$ fixed. When $\beta \geq \frac{3}{4}$, the trajectory would be essentially governed by Eq. (1a) alone with y frozen at $y=y_0$; see Ref. 33.

B. Coherence resonance: $\varepsilon^{3/2}|\mu|^{3/2} \ln^{-1/2}\varepsilon^{-1} \lesssim \delta \ll 1$, $\delta_1 \ll \ln^{-1/2}\varepsilon^{-1}$

When $\delta_2=0$ and the value of δ_1 is decreased, the SISR limit cycle crosses over to the deterministic limit cycle created at $a=1^-$ in the limit $\varepsilon \to 0$, with period $T_{\mathrm{SISR}}(1,0)\simeq 3$, corresponding to the CR limit cycle.[21] This is the case in which $\varepsilon^{3/2}|\mu|^{3/2}\ln^{-1/2}\varepsilon^{-1} \ll \delta_1 \ll \ln^{-1/2}\varepsilon^{-1}$, with $\mu<0$ and $\varepsilon^{-1/2} \lesssim |\mu| \ll \varepsilon^{-1}$. Alternatively, the CR limit cycle is created when $\delta_1=0$ and $\varepsilon^{3/2}|\mu|^{3/2}\ln^{-1/2}\varepsilon^{-1} \lesssim \delta_2 \ll 1$ for these values of μ. To extend these results to the case of $|\mu| \lesssim \varepsilon^{-1/2}$, we simply observe that the noise always overwhelms the dynamics governed by Eqs. (8a) and (8b) for $\delta \gtrsim \varepsilon^{3/4}$, resulting in a CR limit cycle as well for these values of μ.

C. Transition from sporadic single spikes to clusters of spikes: $-\mu \gtrsim \varepsilon^{-5/4}\delta$, $\varepsilon \lesssim \delta \ll \varepsilon^{3/4}$

Let us first consider the case $\mu<0$ and $1 \ll |\mu| \ll \varepsilon^{-1/2}$. Since we are in the scaling regime in which the results of Sec. III B are applicable, we need to consider the probability of the trajectory "sticking" to the fixed point after arriving in its vicinity. For $|\mu|$ sufficiently large, the term involving b_3 dominates in the expression for b. By examining Eqs. (29) and (30), or, simply estimating r with r_1 from Eq. (31), one can see that the probability of the trajectory falling to the small neighborhood of the fixed point becomes overwhelming when $|\mu| \gg \varepsilon^{-5/4}\delta$. Once the trajectory comes to the vicinity of the fixed point, it needs to overcome the barrier $\Delta V \sim |\mu|$. Hence, since $|\mu| \gg \varepsilon^{-2}\delta^2$ in this range, the trajectory will stay near the fixed point an exponentially long $O[\exp(|\mu|\varepsilon^2/\delta^2)]$ time before escaping and undergoing a single large excursion (a spike). Upon returning to the vicinity of the fixed point, this situation will repeat. Note that this is also what will happen in the limit $\varepsilon \to 0$, then $\delta \to 0$, for $a=O(1)$ in the excitable regime.

On the other hand, when $\mu<0$ and $|\mu|=O(\varepsilon^{-5/4}\delta)$, a different scenario will occur. Now we will have the probability $1-r$ of the trajectory sticking to the fixed point significantly different from unity. As a result, once a large excursion away from the fixed point occurs, it will be followed by another excursion with probability $r=O(1)$, resulting in a clustering of spikes. Still, if the trajectory goes to the vicinity of the fixed point, it will take a long $O[\exp(|\mu|\varepsilon^2/\delta^2)]$ time to escape, just like before. Thus, this parameter regime is characterized by rare clusters of spikes.

D. Transition from clusters of spikes to bursting relaxation oscillations: $\varepsilon^{-2}\delta^2 \ll -\mu \ll \varepsilon^{-5/4}\delta$, $\varepsilon \lesssim \delta \ll \varepsilon^{3/4}$

From the results of Sec. III B, for $\varepsilon^{-2}\delta^2 \ll |\mu| \ll \varepsilon^{-5/4}\delta$, which implies $1 \lesssim |\mu| \ll \varepsilon^{-1/2}$, we have $r \simeq 1$. This means that with overwhelming probability one large excursion will be followed by another, etc., with only sporadic transitions to no oscillations with an exponentially long lifetime. In other words, in this regime one will observe persistent bursts of relaxation oscillations, alternating with periods of quiescence. In contrast, for $|\mu| \ll \varepsilon^{-2}\delta^2$, the drift term b changes sign, and now we have $r=1$ exactly. When $|\mu|=O(\varepsilon^{-2}\delta^2)$, the lifetime of the fixed point becomes $O(1)$, see Eq. (26), and so the trajectory cannot stick to the fixed point any more. Therefore, in this case we have relaxation oscillations, as in CR. The transition from bursting to the full limit cycle occurs asymptotically at $\mu=\mu^*-\varepsilon^{-2}(\delta_1^2+2\delta_2^2)$, according to Eq. (21).

E. Transition from bursting relaxation oscillations to no oscillations or small-amplitude limit cycle: $\mu=O(1)$, $\varepsilon^{5/4} \ll \delta \ll \varepsilon$

Since the case of large negative μ has already been treated above, throughout the rest of our analysis we will assume that $\mu=O(1)$. Now the terms in b associated with b_1 and b_2 are negligible. Following the arguments above, we may conclude that in the considered scaling one should observe bursting relaxation oscillations for $\mu<\mu^*$. If $\mu<0$, bursting will alternate with periods of quiescence. On the other hand, when $0<\mu<\mu^*$, bursting relaxation oscillations will, in turn, alternate with the small-amplitude limit cycle whose lifetime is still long, $O[\exp(\varepsilon^2/\delta^2)]$ time. For $\mu \geq \mu^*$, one will observe relaxation oscillations. Note that this is the range of parameters in which mixed-mode oscillations (i.e., either small-amplitude limit cycle or relaxation oscillations) will occur.

F. Rare clusters of spikes: $\mu=O(1)$, $\delta=O(\varepsilon^{5/4})$

This is the case in which $r=O(1)$, giving rise to clusters of spikes. As before, if $\mu<0$, these clusters will alternate with the exponentially long stays in the vicinity of the fixed point. If $0<\mu<\mu^*$, the clusters compete with the exponentially long-lived small-amplitude limit cycle. Still, only relaxation oscillations will be observed for $\mu \geq \mu^*$.

G. No oscillations or small-amplitude oscillations plus sporadic single spikes: $\mu=O(1)$, $\delta \ll \varepsilon^{5/4}$

Lastly, when $\delta \ll \varepsilon^{5/4}$, we have $r \simeq 0$ for $\mu<\mu^*$, and so only the deterministic solution (fixed point for $\mu \leq 0$, small-amplitude limit cycle for $0<\mu<\mu^*$, or relaxation oscillations for $\mu \geq \mu^*$) will be observed. Occasionally, on the $O[\exp(\varepsilon^2/\delta^2)]$ time scale, one will see rare single-spike excursions away from the deterministic limit.

V. NUMERICAL SIMULATIONS

We now present the results of the numerical simulations of Eqs. (1a) and (1b) for different levels of the noise, corroborating the conclusions of the asymptotic analysis of the preceding sections. Here we will present a study of the effect of the noise acting on the x variable only, i.e., $\delta_1>0$ and $\delta_2=0$, since this is the case that leads to SISR for sufficiently large δ_1 and is, therefore, the most interesting one. We verified that for smaller δ's, when SISR does not occur, it does not matter where precisely the noise is added, in agreement

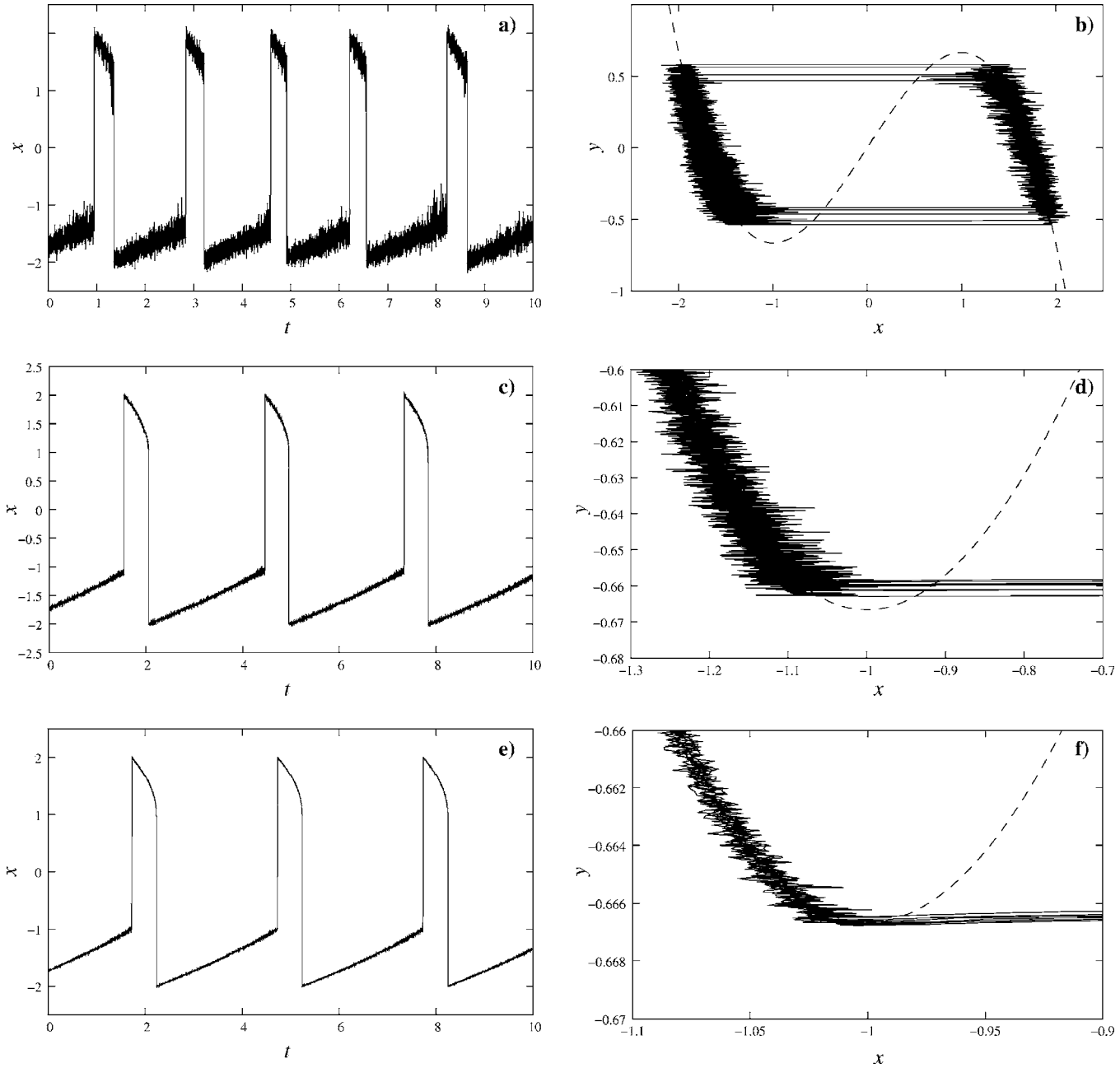

FIG. 6. The transition from the SISR limit cycle to the CR limit cycle as the noise amplitude is decreased. Results of the numerical solution of Eqs. (1a) and (1b) with $\varepsilon=10^{-4}$, $1-a=10^{-5}$, $\delta_2=0$, and different values of δ_1. In (a,c,e) the time series of x is shown, and in (b,d,f) the phase portrait is plotted. The values of δ_1 are $\delta_1=0.2$ in (a,b), $\delta_1=0.02$ in (c,d), and $\delta_1=0.002$ in (e,f).

with our asymptotic analysis of the preceding sections. In all cases, Eqs. (1a) and (1b) were discretized using a simple Euler scheme with the time step $\Delta t=0.01\varepsilon$ to ensure that the shortest time scale in the problem is adequately resolved. The noise was generated using the standard Box-Muller algorithm based on the lagged Fibonacci pseudorandom number generator (see, e.g., Ref. 36; the implementation is available at NETLIB, www.netlib.org).

Throughout the simulations below, we fix $\varepsilon=10^{-4}$ and $a=1-0.1\varepsilon$ at which a small-amplitude limit cycle exists in the system for $\delta=0$. We first choose the noise amplitude in the range of the validity of SISR, $\delta_1=0.2$, see Ref. 21. The results of the simulations are shown in Figs. 6(a) and 6(b). One can clearly see a coherent noise-induced limit cycle due to SISR. We then observe the changes in the dynamics as the value of δ_1 is decreased by an order of magnitude. When $\delta_1=0.02$, the limit cycle becomes considerably more coherent, Fig. 6(c), yet the period and other parameters of oscillations are still determined by SISR, with the jump-off point approaching the left knee on S_L, Fig. 6(d). This is consistent with the explanation of Ref. 21 as the value of a approaches the bifurcation threshold. Upon further decrease to $\delta_1=0.002$, one obtains a quasideterministic precursor to the large-amplitude relaxation limit cycle, Figs. 6(e) and 6(f), created at $a\to 1^-$ in the limit $\varepsilon\to 0$. This is the parameter regime in which the limit cycle due to SISR becomes indistinguishable from the one due to CR.[14,21] The sequence of

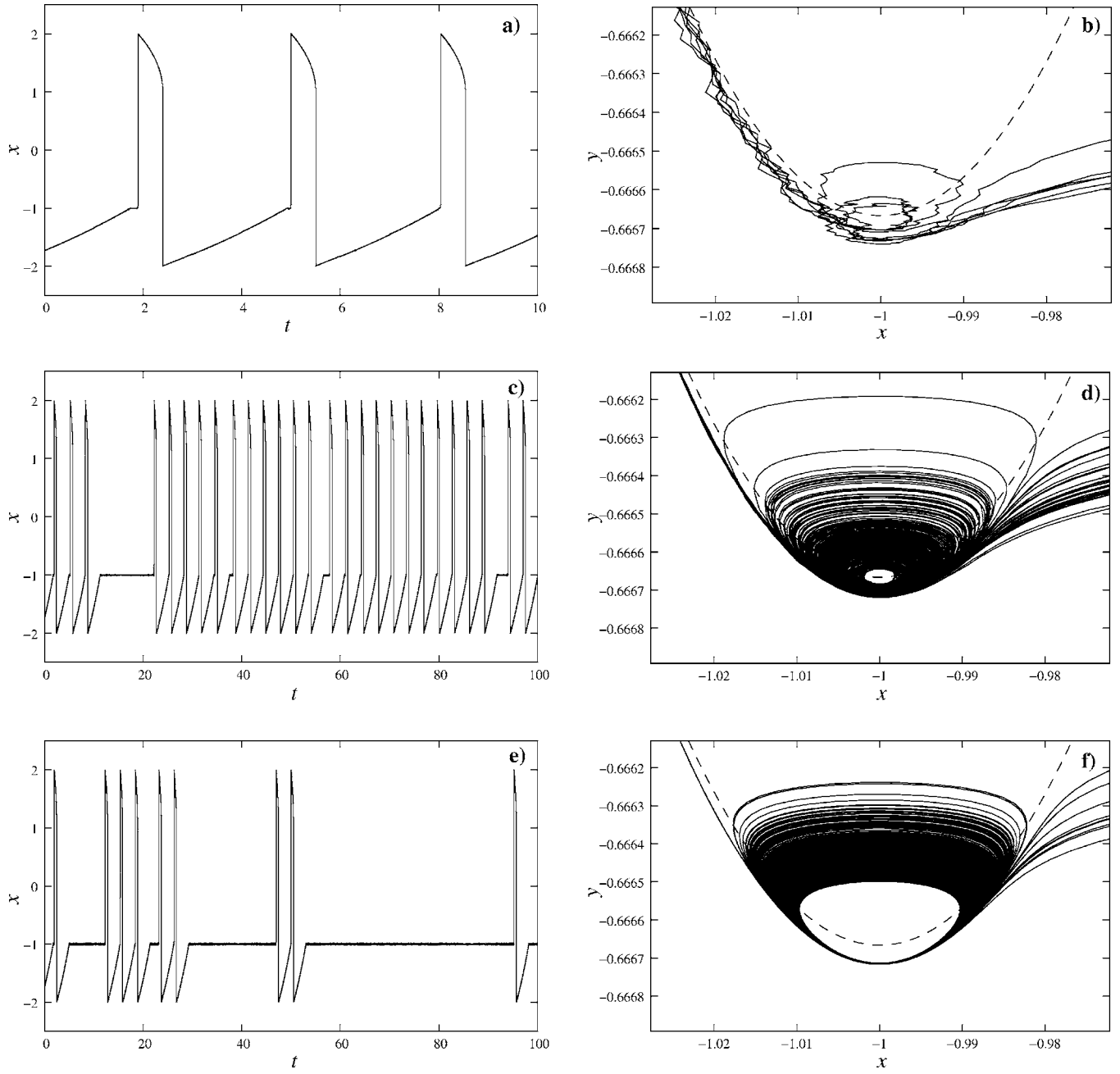

FIG. 7. The transition from the relaxation limit cycle to the small-amplitude limit cycle as the noise amplitude is decreased further. Results of the numerical solution of Eqs. (1a) and (1b) with $\varepsilon=10^{-4}$, $1-a=10^{-5}$, $\delta_2=0$, and different values of δ_1. In (a,c,e) the time series of x is shown, and in (b,d,f) the phase portrait is plotted. The values of δ_1 are $\delta_1=2\times10^{-4}$ in (a,b), $\delta_1=2\times10^{-5}$ in (c,d), and $\delta_1=2\times10^{-6}$ in (e,f).

transitions just observed corresponds to the situation in which $\delta\gtrsim\varepsilon^{3/4}$, discussed in Sec. IV.

This picture begins to change qualitatively as the value of δ_1 is decreased further. When $\delta_1=2\times10^{-4}=0.2\varepsilon^{3/4}$, one still observes a coherent large-amplitude relaxation limit cycle, Fig. 7(a). However, now the trajectory loops around a few times before exiting the neighborhood of the fixed point, see Fig. 7(b). One can also see a small delay in the transition from S_L to S_R in Fig. 7(a). This effect becomes considerably more pronounced for $\delta_1=2\times10^{-5}=0.2\varepsilon$ when the trajectory typically makes several highly coherent loops around the fixed point at every cycle, see Figs. 7(c) and 7(d). Occasionally, the trajectory gets attracted to the small-amplitude limit cycle; it can then take a long time for a system to escape and perform a large excursion. This is the regime in which bursts of relaxation oscillations are observed, alternating with the small-amplitude limit cycle. As the value of δ_1 is decreased even further to $\delta_1=2\times10^{-6}=0.2\varepsilon^{5/4}$, the character of the observed dynamics changes yet again, see Figs. 7(e) and 7(f). Now, the trajectory is typically attracted to the small-amplitude limit cycle, Fig. 7(f). Occasionally, the noise pushes the system outside the basin of attraction of the limit cycle, giving rise to clusters of several relaxation cycles (spikes), see Fig. 7(e). From the simulations, the probability of one spike following another within the time interval $\Delta t\leq6$ is $r\simeq0.73$, in agreement with the asymptotic result ob-

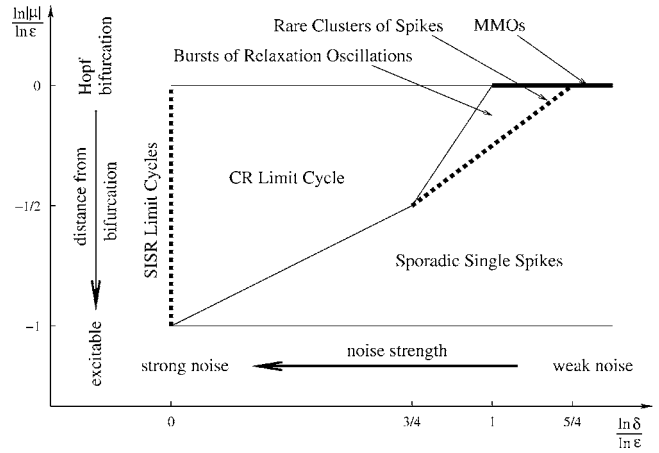

FIG. 8. The diagram of different scaling regimes near singular Hopf bifurcation. The boundary between CR and sporadic single spikes is where $-\mu \sim \varepsilon^{-1}\delta^{2/3}$. The boundary between CR and bursting is where $-\mu \sim \varepsilon^{-2}\delta^2$, and the boundary between bursting and sporadic single spikes is where $-\mu \sim \varepsilon^{-5/4}\delta$. Note that for SISR to occur, the noise associated with δ_1 must dominate.

tained numerically for this set of parameters at the end of Sec. III B.

Finally, as the noise amplitude is decreased further, the spikes quickly become exceedingly rare and essentially are not observed any more. This is the regime in which the deterministic dynamics, i.e., the small-amplitude limit cycle for these values of the parameters, takes over on the time scale of the observation (results not shown). Note that all the transitions discussed above and the associated scales of the noise amplitude are consistent with the predictions of the asymptotic analysis of Sec. IV.

VI. SUMMARY AND DISCUSSION

Let us now summarize our findings. We have considered a two-variable dynamical system that exhibits relaxation oscillations, as well as a singular Hopf bifurcation, in the limit of strong timescale separation. We found that Gaussian white noise of small amplitude significantly modifies the observed dynamics near the Hopf bifurcation, giving rise to new phenomena: bursting relaxation oscillations and spike clustering, as well as modifying the parameter ranges in which no oscillations, small-amplitude limit cycle, or relaxation limit cycle are observed.

We performed an asymptotic analysis of the dynamics in the limit of strong timescale separation, $\varepsilon \to 0$, under various scalings of δ and $\mu=\varepsilon^{-1}(1-a)$ with ε. The results of our analysis can be conveniently summarized in the scaling diagram presented in Fig. 8. This figure shows different scaling regions of the dynamics in the $(\ln \delta/\ln \varepsilon)-(\ln|\mu|/\ln \varepsilon)$ plane. Our previous analysis covered the case of SISR, which in Fig. 8 is represented by the thick dashed line at $\delta_1=O(\ln^{-1/2}\varepsilon^{-1})$, independently of μ, as well as the case of CR for $\varepsilon^{-1/2} \ll \mu \ll \varepsilon^{-1}$ and $\varepsilon^{3/2}|\mu|^{3/2}\ln^{-1/2}\varepsilon^{-1} \lesssim \delta \ll 1$, see Ref. 21. Our present analysis covers the region $|\mu| \ll \varepsilon^{-1/2}$ and $\delta \ll \varepsilon^{3/4}$.

We found that the relaxation limit cycle due to CR persists for $-\mu \lesssim \varepsilon^{-2}\delta^2$ and $\delta \gg \varepsilon$. In the region $\varepsilon^{5/4} \ll \delta \ll \varepsilon^{3/4}$ and $\varepsilon^{-2}\delta^2 \ll -\mu \ll \varepsilon^{-5/4}\delta$, one will, instead, see bursts of relaxation oscillations, alternating with periods of quiescence in which the system remains near the stable fixed point. When $\mu<0$ and $|\mu|=O(\varepsilon^{-5/4}\delta)$, one will see clusters of several relaxation cycles (spikes) separated by long periods of quiescence. Finally, only sporadic single spikes can be excited by the noise for $\delta \ll \varepsilon^{5/4}|\mu|$, for all $-\mu \gtrsim 1$. Let us note that the intervals of bursts and of quiescence between spikes must follow asymptotically a Poisson distribution with exponentially long lifetimes.[33] This is in contrast with the sharply peaked interspike interval distribution due to SISR.[21]

Finally, mixed-mode oscillations (MMOs) are observed in the considered system for $\mu=O(1)$. Here one can separate four different regimes. First, when $\delta_1=O(\ln^{-1/2}\varepsilon^{-1})$ and $\delta_2 \ll 1$, one will observe the noise-induced limit cycle due to SISR.[18,21,22] Then, at $\varepsilon \ll \delta \ll 1$ the CR relaxation limit cycle emerges. This crosses over at $\varepsilon^{5/4} \ll \delta \ll 1$ to bursts of relaxation oscillations alternating with long periods of quiescence when $\mu<0$, or with long-lived small-amplitude oscillations, if $0<\mu<\mu^*$. Still, relaxation oscillations persist asymptotically when $\mu>\mu^*$. At $\delta=O(\varepsilon^{5/4})$, spike clustering will be observed for $\mu<\mu^*$. Finally, when $\delta \ll \varepsilon^{5/4}$, the observed dynamics is essentially described by the deterministic version of Eqs. (1a) and (1b), with rare isolated spikes due to noise.

Let us now see how all this picture affects the slow passage through the Hopf bifurcation in the considered problem. Up to now we were studying the effect of varying noise amplitude on the system with fixed deterministic parameters. A more realistic question is what happens with the system at fixed timescale ratio $\varepsilon \ll 1$ and noise amplitude $\delta \ll 1$ as the value of the control parameter μ passes adiabatically through the bifurcation threshold ($\mu=0$). Here the following four scenarios are possible. First, if the values of δ and ε obey the scaling of SISR, then the deterministic Hopf bifurcation at $\mu=0$ has little to do with the observed stochastic bifurcation at $-\mu=O(\varepsilon^{-1})$, see Refs. 21 and 22. Alternatively, suppose we fix $\delta=O(\varepsilon^{\alpha})$ with $\alpha \in (0, \frac{3}{4})$. Then upon passing through the bifurcation point, an abrupt transition to the relaxation limit cycle will occur at $-\mu \gg \varepsilon^{-1/2}$ by the CR mechanism, before the deterministic threshold. If, on the other hand, $\alpha \in (\frac{3}{4}, \frac{5}{4})$, then, first, isolated spikes will appear, followed by clusters of spikes, at $-\mu=O(\varepsilon^{-5/4+\alpha})$. As the value of μ is increased further, the clusters of spikes will become more numerous, transforming into bursts of relaxation oscillations. These bursts eventually become continuously firing when $-\mu$ reaches $O(\varepsilon^{2(\alpha-1)})$ if $\alpha<1$. For $\alpha>1$, on the other hand, bursting continues up to $\mu=O(1)$, and so the character of interburst intervals will change from no oscillations to small-amplitude oscillations when μ reaches zero. After that, the interburst intervals will become progressively shorter, until at $\mu=\mu^*$ continuous firing is established. The latter is illustrated by a numerical simulation in Fig. 9. Finally, if $\alpha>\frac{5}{4}$, then the observed sequence of transitions will essentially coincide with the bifurcation diagram of the deterministic system; noise will become mostly negligible in this regime.

In conclusion, let us note that the dynamics uncovered by our analysis should not rely on the details of the particular model studied in this paper and are, therefore, expected to be

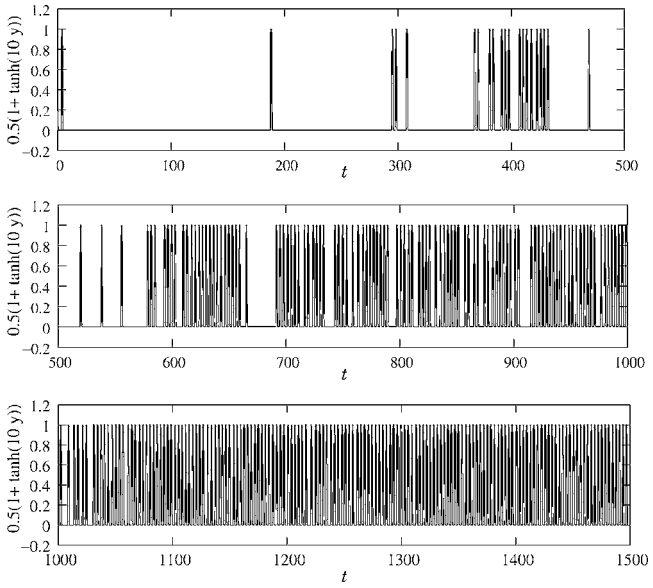

FIG. 9. A slow passage through the Hopf bifurcation. Result of the numerical solution of Eqs. (1a) and (1b) with $\varepsilon=10^{-4}$, $\delta=2\times10^{-6}$, and a ramped linearly from $a=1-0.075\varepsilon$ to $a=1-0.15\varepsilon$ over the simulation window.

observed in generic excitable systems with strong separation of time scale. Such systems are abundant in applications, especially in biology. We point out that the phenomena of spike clustering and bursting oscillations in models of relaxation oscillators near a singular Hopf bifurcation in the presence of noise, which describe systems of very different physical nature, were first observed in Refs. 15, 16, 37, and 38. These phenomena are also widely observed experimentally (see, e.g., Refs. 4 and 39). Our analysis suggests that the possible constructive role of noise should be carefully considered in the modeling of these phenomena.

The mechanism of mixed-mode oscillations analyzed by us should also persist in more complicated models containing more than two degrees of freedom. These types of models may introduce an interesting interplay between the stochastic effects and several slow variables. In particular, such systems may self-tune in a way that the slow dynamics continuously brings the trajectory to the neighborhood of the shadow of the Hopf bifurcation, where the effect of small noise can be significant.[15,40] Let us note that the effect of spike clustering was observed in the simulations of a detailed biophysical model of medial entorhinal cortex layer II stellate cells in the presence of small noise.[41] A recent analytical study[42] revealed a lower-dimensional reduction of the full model in Ref. 41 that has the ingredients necessary for the mechanism discussed in this paper to be feasible.

ACKNOWLEDGMENTS

One of the authors (C.B.M.) would like to acknowledge useful discussions with A. M. Berezhkovskii. This work was supported, in part, by National Institute of Health Grant No. R01 GM076690 (C.B.M.), National Science Foundation Grant Nos. DMS02-09959 and DMS02-39625, and Office of Naval Research Grant No. N00014-04-1-0565 (E.V.-E.).

[1] J. Guckenheimer and P. Holmes, *Nonlinear Oscillations, Dynamic Systems, and Bifurcations of Vector Fields* (Springer-Verlag, New York, 1983).
[2] *Oscillations and Traveling Waves in Chemical Systems*, edited by R. J. Field and M. Burger (Wiley Interscience, New York, 1985).
[3] A. Goldbeter, *Biochemical Oscillations and Cellular Rhythms* (Cambridge University Press, Cambridge, 1996).
[4] C. Koch, *Biophysics of Computation* (Oxford University Press, Oxford, 1999).
[5] J. Keener and J. Sneyd, *Mathematical Physiology* (Springer-Verlag, New York, 1998).
[6] E. F. Mishchenko, Y. S. Kolesov, A. Y. Kolesov, and N. K. Rozov, *Asymptotic Methods in Singularly Perturbed Systems, Monographs in Contemporary Mathematics* (Consultants Bureau, New York, 1994).
[7] B. van der Pol, Philos. Mag. **2**, 978 (1926).
[8] A. A. Andronov, A. A. Vitt, and S. E. Khaikin, *Theory of Oscillators*, translated from the Russian by F. Immirzi; translation edited and abridged by W. Fishwick (Pergamon, Oxford, 1966).
[9] J. Grasman, *Asymptotic Methods for Relaxation Oscillations and Applications* (Springer, Berlin, 1987).
[10] A. Goldbeter, Nature (London) **420**, 238 (2002).
[11] H.-S. Hahn, A. Nitzan, P. Ortoleva, and J. Ross, Proc. Natl. Acad. Sci. U.S.A. **71**, 4067 (1974).
[12] J. M. G. Vilar, H. Y. Kueh, N. Barkai, and S. Leibler, Proc. Natl. Acad. Sci. U.S.A. **99**, 5988 (2002).
[13] A. Longtin, Phys. Rev. E **55**, 868 (1997).
[14] A. S. Pikovsky and J. Kurths, Phys. Rev. Lett. **78**, 775 (1997).
[15] V. V. Osipov and E. V. Ponizovskaya, Phys. Lett. A **238**, 369 (1998).
[16] V. V. Osipov and E. V. Ponizovskaya, JETP Lett. **70**, 425 (1999).
[17] M. I. Freidlin, J. Stat. Phys. **103**, 283 (2001).
[18] C. B. Muratov, E. Vanden-Eijnden, and W. E, Physica D **210**, 227 (2005).
[19] N. Berglund and B. Gentz, *Noise-Induced Phenomena in Slow-Fast Dynamical Systems. A Sample-Paths Approach* (Springer-Verlag, Berlin, 2005).
[20] B. Lindner, J. Garcia-Ojalvo, A. Neiman, and L. Schimansky-Geier, Phys. Rep. **392**, 321 (2004).
[21] R. E. Lee DeVille, E. Vanden-Eijnden, and C. B. Muratov, Phys. Rev. E **72**, 031105 (2005).
[22] R. E. Lee DeVille, C. B. Muratov, and E. Vanden-Eijnden, J. Chem. Phys. **124**, 231102 (2006).
[23] C. B. Muratov, E. Vanden-Eijnden, and W. E, Proc. Natl. Acad. Sci. U.S.A. **104**, 702 (2007).
[24] R. E. L. DeVille and E. Vanden-Eijnden, Nonlinearity **20**, 51 (2007).
[25] R. E. L. DeVille and E. Vanden-Eijnden, J. Stat. Phys. **126**, 75 (2007).
[26] S. M. Baer and T. Erneux, SIAM J. Appl. Math. **46**, 721 (1986).
[27] S. M. Baer and T. Erneux, SIAM J. Appl. Math. **52**, 1651 (1992).
[28] S. M. Baer, T. Erneux, and J. Rinzel, SIAM J. Appl. Math. **49**, 55 (1989).
[29] B. Braaksma, J. Nonlinear Sci. **8**, 457 (1998).
[30] T. Tateno and K. Pakdaman, Chaos **14**, 511 (2004).
[31] E. Benoit, J. F. Callot, F. Diener, and M. Diener, Collect. Math. **32**, 37 (1981).
[32] W. Eckhaus, *Asymptotic Analysis, II,* Vol. 985 of Lecture Notes in Mathematics (Springer, Berlin, 1983), pp. 449–494.
[33] M. I. Freidlin and A. D. Wentzell, *Random Perturbations of Dynamical Systems*, 2nd ed. (Springer, New York, 1998).
[34] C. W. Gardiner, *Handbook of Stochastic Methods for Physics, Chemistry, and the Natural Sciences* (Springer-Verlag, New York, 1997).
[35] V. A. Makarov, V. I. Nekorkin, and M. G. Velarde, Phys. Rev. Lett. **86**, 3431 (2001).
[36] M. Mascagni, S. A. Cuccaro, D. V. Pryor, and M. L. Robinson, J. Comput. Phys. **119**, 211 (1995).
[37] V. V. Osipov and E. V. Ponizovskaya, J. Commun. Technol. Electron. **43**, 630 (1998).
[38] V. V. Osipov and E. V. Ponizovskaya, J. Commun. Technol. Electron. **43**, 186 (1998).
[39] J. A. White, R. Klink, A. Alonso, and A. R. Kay, J. Neurophysiol. **80**, 262 (1998).
[40] V. V. Osipov and E. V. Ponizovskaya, Phys. Lett. A **271**, 191 (2000).
[41] E. Fransen, A. A. Alonso, C. T. Dickson, J. Magistretti, and M. E. Hasselmo, Hippocampus **14**, 368 (2004).
[42] H. G. Rotstein, T. Oppermann, J. A. White, and N. Kopell, J. Comput. Neurosci. **21**, 271 (2006).